ChemComm

COMMUNICATION

View Article Online
View Journal | View Issue

Cite this: *Chem. Commun.*, 2023, **59**, 1525

Received 4th December 2022,
Accepted 12th January 2023

DOI: 10.1039/d2cc06601g

rsc.li/chemcomm

Benzophenone-containing phosphors with an unprecedented long lifetime of 1.8 s under ambient conditions†

Yuming Su,[ab] Minjian Wu,[b] Guangming Wang,[b] Jiuyang Li,[b] Xuefeng Chen,[b] Xun Li,[b] Guoxiang Wang*[a] and Kaka Zhang *[b]

It is well-known that benzophenone has a short phosphorescence lifetime of around 1 ms even at 77 K. Here we report a benzophenone-containing emitter with an unprecedented long phosphorescence lifetime of 1.8 s under ambient conditions, which can be attributed to its T_1 state of localized excitation nature as revealed by detailed studies.

Manipulation of triplet excited states is of vital importance for fabricating high-performance room-temperature phosphorescence (RTP) materials.[1–17] In organic systems, due to the spin-forbidden nature of the triplet population, transformation and decay, it is challenging to construct highly efficient and long-lived RTP materials under ambient conditions. Intersystem crossing and phosphorescence decay represent two of the most important photophysical processes in organic RTP systems, with rate constants of k_{ISC} and k_P, respectively. Diverse strategies have been developed to enhance k_{ISC} or k_P or both to increase RTP efficiency or RTP lifetime.[18–25] Among these strategies, the heavy atom effect (HAE) and the introduction of n–π* transitions are the mostly used and very reliable methods to enhance both k_{ISC} and k_P.[26–31] For example, the internal HAE and external HAE have been reported to promote spin–orbit coupling, and facilitate S_1-to-T_1 ISC and T_1-to-S_0 phosphorescence.[26–29] In some circumstance, the RTP efficiency can exceed 50%. The involvement of n–π* transition characters has been reported to reduce the fluorescence decay rate (k_F), which is helpful for organic systems to achieve high Φ_{ISC}.[30,31] On the other hand, T_1 states with n–π* characters show large k_P to harvest triplet energies. Despite the advantages of the triplet population and harvesting, the strategies based on HAE and n–π* transition show severe side effects of reducing the RTP lifetimes (τ_P).

The long-lived excited states are the defining characters of RTP materials, which endow the opportunity for their application in various fields.[1–17] The present study focuses on RTP lifetimes in benzophenone-containing systems. It is known that benzophenone has high Φ_{ISC} close to unity because of two reasons. (1) The S_1 state of benzophenone shows typical n–π* character and has small k_F around 10^6 s^{-1}. (2) The T_2 state of π–π* character has an energy level close to the S_1 state of n–π* character; according to the energy gap law and the El-Sayed rule, the S_1-to-T_2 ISC is very fast with k_{ISC} around 10^{11} s^{-1}. However, benzophenone's T_1 state is also of n–π* character to exhibit large k_P and thus short RTP lifetime. Actually, even at low temperatures such as 77 K where nonradiative decay of the T_1 state is sufficiently suppressed, the phosphorescence lifetime of benzophenone is still around 1 ms. To increase the RTP lifetimes, various benzophenone-containing systems have been reported, some of which exhibit RTP lifetimes longer than 0.1 s.[4,20,32–34] The balance of RTP efficiency and RTP lifetime has also been sufficiently discussed in a recent study.[31] It is found that most of the reported benzophenone-containing materials are based on single-component systems, with two-component systems being rarely explored. In addition, the RTP lifetimes in the reported benzophenone-containing systems are mostly several hundred ms or around 0.5 s. It remains a formidable task to achieve long RTP lifetimes in benzophenone-containing systems, for example, 0.8 s, 1.0 s and even longer.

Here, we report the fabrication of a series of benzophenone-containing materials *via* a dopant-matrix strategy; benzophenone-containing compounds **1** to **6** are used as luminescent dopants while phenyl benzoate (PhB) serves as the organic matrix (Fig. 1). It is found that **1**-PhB and **2**-PhB materials show RTP properties, but have insignificant room-temperature afterglow (τ_P around 1 ms or several ms). **3**-PhB, **4**-PhB and **5**-PhB materials exhibit afterglow with τ_P of several hundred ms under ambient conditions.

[a] *School of Chemistry and Chemical Engineering, Hunan Institute of Science and Technology, People's Republic of China. E-mail: 11991397@hnist.edu.cn*
[b] *Key Laboratory of Synthetic and Self-Assembly Chemistry for Organic Functional Molecules, Shanghai Institute of Organic Chemistry, University of Chinese Academy of Sciences, Chinese Academy of Sciences, 345 Lingling Road, Shanghai 200032, People's Republic of China. E-mail: zhangkaka@sioc.ac.cn*

† Electronic supplementary information (ESI) available. See DOI: https://doi.org/10.1039/d2cc06601g

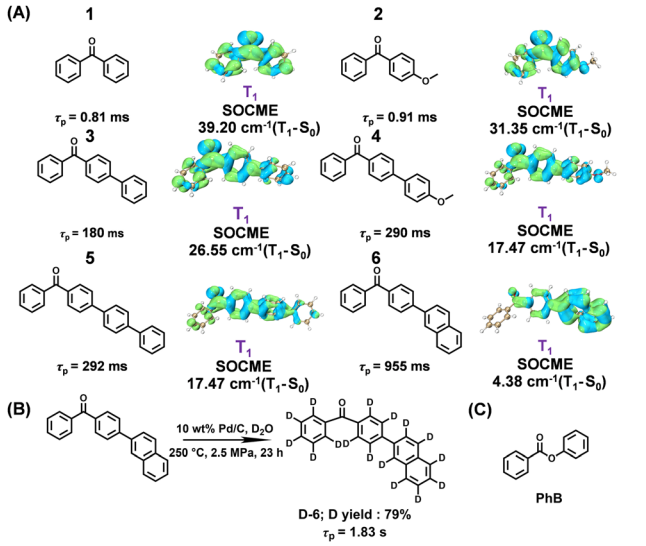

Fig. 1 (A) Chemical structures of benzophenone-containing compounds **1** to **6**, their RTP lifetimes after doping into the PhB matrix, the electron–hole density difference of their T_1 states, and the T_1 to S_0 SOCME values. (B) Random deuteration of **6** and the unprecedented long lifetime of 1.8 s of deuterated **6**-PhB materials under ambient conditions. (C) Chemical structures of PhB.

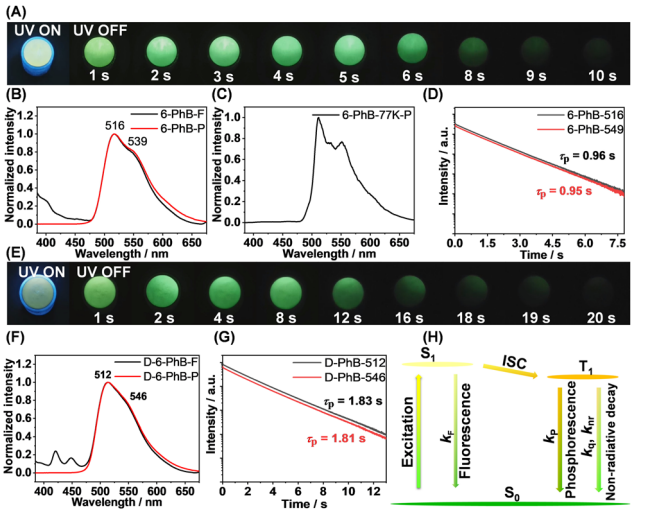

Fig. 2 (A) Photographs of **6**-PhB materials under UV lamp and after ceasing the UV lamp. (B) Room-temperature steady-state and delayed emission spectra of **6**-PhB materials. (C) 77 K delayed emission spectra of **6**-PhB materials. (D) Room-temperature phosphorescence decay of **6**-PhB materials. (E) Photographs of deuterated **6**-PhB materials under UV lamp and after ceasing the UV lamp. (F) Room-temperature steady-state and delayed emission spectra of deuterated **6**-PhB materials. (G) Room-temperature phosphorescence decay of deuterated **6**-PhB materials. (H) Proposed RTP mechanism of **6**-PhB materials.

Interestingly, **6**-PhB materials have been found to display ultralong τ_P close to 1 s. Furthermore, after deuteration of **6**, the deuterated **6**-PhB materials exhibit τ_P up to 1.8 s, which is among the longest values in the reported benzophenone-containing systems.[30–34] TD-DFT calculations show that the component of localized excitation in the T_1 states increases from **1**-PhB to **6**-PhB, which is in line with the increase of τ_P from **1**-PhB to **6**-PhB (Fig. 1).

The synthetic procedures and structural characterization of the benzophenone-containing compounds **1–6** and deuterated **6** are attached in the ESI.† Solution UV-vis measurements and TD-DFT calculations show that the lower-energy absorption bands of compounds **1–6** at around 350 nm can be assigned as S_0 to S_1 transitions of mainly n–π* excitation characters, while the intense higher-energy bands can be attributed to S_0 to S_n ($n \geq 2$) transitions of π–π* or intramolecular charge transfer (ICT) characters (Table S1 and Fig. S1–S8, ESI†). **1–6** solids under ambient conditions show insignificant room-temperature afterglow ($\tau_P < 0.1$ s) (Fig. S9, ESI†).

We apply the dopant-matrix strategy to fabricate afterglow materials and select the electronically inert PhB matrix to accommodate luminescent dopants. It is found that **1**-PhB and **2**-PhB materials still don't show room-temperature afterglow, while **3**-PhB to **6**-PhB materials exhibit significant room-temperature afterglow that can last for 2 to 10 seconds in a dark room (Table S2, Fig. S10–S15, ESI† and Fig. 2A). Table S2 (ESI†) summarizes the photophysical data of these materials, among which the **6**-PhB materials display very long afterglow lifetimes. The **6**-PhB materials at room-temperature show a minor band in the range of 390 nm to 470 nm and a major band ranging from 470 nm to 650 nm (Fig. 2B) in their steady-state emission spectra. Their delayed emission spectra (1 ms delay) at room temperature are found to coincide with the 470–650 nm major band of the steady-state spectra, both of which exhibit emission maxima at 516 nm and a shoulder at 539 nm (Fig. 2B). Low temperature delayed emission spectra (1 ms delay) at 77 K display a clearly resolved phosphorescence band (Fig. 2C), which locates in the same region as the room-temperature delayed emission band (Fig. 2B). These results suggest that the 470–650 nm major band originates from phosphorescence, while the 390–470 nm minor band can be assigned as fluorescence (Fig. 2B); such kind of steady-state emission spectra indicate high Φ_{ISC} in the **6**-PhB system.

The phosphorescence decay of **6**-PhB materials follows single-exponential decay with RTP lifetimes of 0.96 s (Fig. 2D). It is known that deuteration of RTP molecules can reduce intramolecular motions and nonradiative decay of triplet states;[35–37] the vibration of C–D bonds is much weaker than C–H bonds. However, deuteration of benzophenone-containing RTP molecules has been rarely reported. Here we perform deuteration of **6** to enhance the emission (Text S1, ESI†) and elongate the RTP lifetimes of **6**-PhB systems (Fig. 1B). The deuterated **6**-PhB materials show similar delayed emission spectra (Fig. 2F), while the RTP lifetimes from the phosphorescence decay profile are found to reach 1.8 s (Fig. 2G and Text S1, ESI†), which is among the longest values in the reported benzophenone-containing systems.

To investigate the afterglow mechanism in **6**-PhB systems, several mechanisms should be ruled out. First, the reported studies showed that excited state energy transfer from matrix to dopant can give rise to room-temperature afterglow.[38–40] This is not the case in **6**-PhB afterglow systems excited by 350 nm light,

because the PhB matrix cannot be excited by 350 nm light to serve as the donor of energy transfer (Fig. S16, ESI†). Second, PhB (HOMO = −6.96 eV, LUMO = −1.79 eV) has lower-lying HOMO and higher-lying LUMO than **6** (HOMO = −5.86 eV, LUMO = −1.84 eV), so the organic long persistent luminescence mechanism,[41] which is based on intermolecular charge transfer between matrix and dopant, is not responsible for the afterglow in the **6**-PhB system (Fig. S17, ESI†). Third, PhB's T_1 levels are higher than **6**'s S_1 and T_1 levels, so the afterglow mechanism based on the matrix's T_1 mediation[13,42] is also not responsible for **6**-PhB's afterglow (Fig. S18, ESI†). Fourth, HPLC of **6** and the match of the UV-vis/excitation spectra of the **6** systems can reject an impurity mechanism (Fig. S19 and S20, ESI†).[43] Fifth, a thermally activated delayed fluorescence mechanism,[44–47] which can also lead to room-temperature afterglow, has been ruled out by the low temperature delayed emission studies (Fig. 2C). Based on the above experiments and analyses, we propose that, upon excitation, singlet excited states of **6** form and subsequently undergo efficient ISC to reach triplet excited states (Fig. 2H). The PhB matrix suppresses nonradiative decay of **6**'s T_1 and protects **6**'s T_1 from oxygen quenching. The phosphorescence decay of **6**'s T_1 in the rigid PhB matrix gives rise to the long-lived RTP of the **6**-PhB materials under ambient conditions.

To further understand the triplet population and decay and the long-lived RTP property, we performed theoretical studies on the excited states of the **6** systems. TD-DFT calculations (Fig. 3) show that there are rich S_1 to T_n channels with large spin–orbit coupling matrix elements (SOCMEs), which is consistent with the highly efficient intersystem crossing in the **6** systems. It is interesting to find that **6**'s T_1 state has significant localized excitation (LE) character of the naphthalene group and small n–π* character of the benzophenone group, exhibiting T_1 to S_0 SOCME of only 4.38 cm^{-1} (Fig. 3 and 1A). In striking contrast, the T_1 states of **1**–**5** show significant n–π* characters of the benzophenone groups with SOCME above 17 cm^{-1} (Fig. 1A). It is known that the k_P values of ^{3}n–π* states are much larger than those of ^{3}LE states, so it is understandable that **6**-PhB materials possess much longer RTP lifetimes than the **1**-PhB to **5**-PhB materials. These results indicate the important role of the manipulation of triplet excited states for fabricating high-performance RTP materials.

In view of the long RTP lifetimes and the excellent processability of the PhB matrix, the **6**-PhB materials are selected for the demonstration of the functions of afterglow materials. The **6**-PhB materials can be readily processed into fruit-shaped objects by melt casting with the aid of silicone molds (Fig. 4A). The **6**-PhB materials can also be processed into aqueous afterglow dispersions in the presence of Pluronic F127 surfactant (Fig. 4C). Preliminary bioimaging studies in living fish show that the afterglow imaging mode has very clean background and can avoid the fluorescence interference (Fig. 4D). The **6**-PhB materials have also been found to serve as a donor for energy transfer to fabricate long-lived red afterglow materials. By introducing rhodamine 6G (R6G) into the

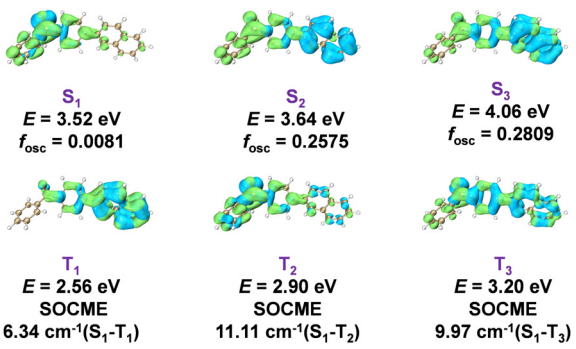

Fig. 3 Iso-surface maps of the electron–hole density difference of **6**'s S_n and T_n states calculated in Gaussian 16 by TD-DFT/B3LYP/6-31G(d,p), where blue and green iso-surfaces correspond to hole and electron distributions, respectively, and SOCME values calculated on ORCA 4.2.1 by TD-DFT/B3LYP/def2-TZVP(-f).

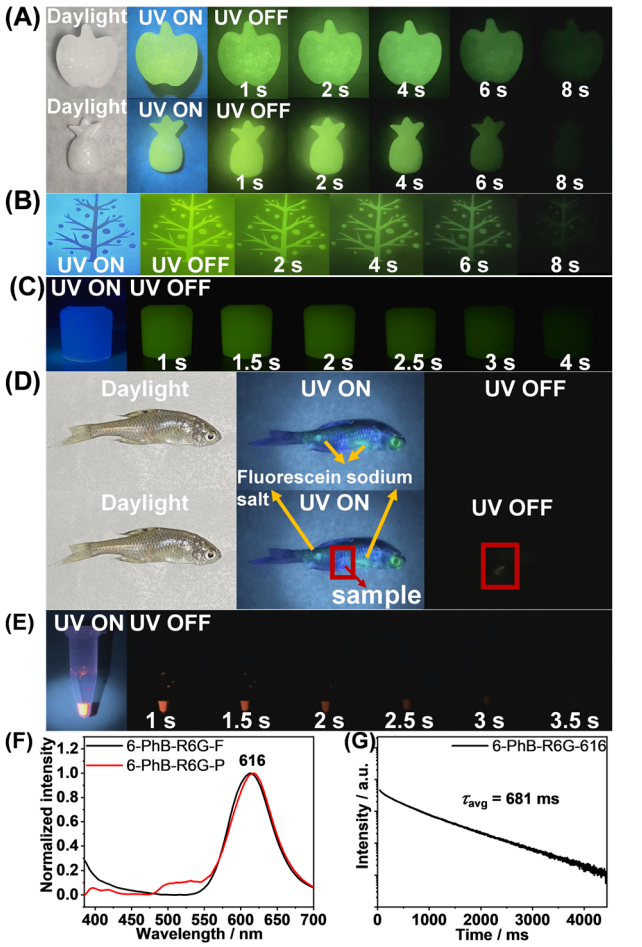

Fig. 4 (A) Photographs of the fruit-shaped afterglow objects of **6**-PhB materials. (B) Photographs of the Christmas tree pattern based on an afterglow film by UV excitation through a pre-designed mask and after removal of the UV lamp. (C) Photographs of the aqueous afterglow dispersion of **6**-PhB materials under UV and after ceasing UV. (D) Preliminary bioimaging studies in living fish with the interference of fluorescence dyes. (E) Photographs of **6**-PhB-R6G three-component materials under UV and after removal of UV excitation. (F and G) Steady-state and delayed emission spectra and afterglow decay of **6**-PhB-R6G materials.

6-PhB system, the resultant three-component materials exhibit red afterglow (Fig. 4E) under ambient conditions with a delayed emission band at 616 nm (Fig. 4F) and afterglow lifetime up to 681 ms (Fig. 4G and Fig. S21, ESI†). This provides an indirect pathway to achieve red afterglow materials, which can bypass the restriction of the energy gap law in directly constructing red RTP materials.

In conclusion, unlike the short RTP lifetimes reported in the benzophenone system, the present study exhibits a benzophenone-containing emitter with unprecedented long phosphorescence lifetime of 1.8 s under ambient conditions. Experimental and theoretical studies reveal that the **6**-PhB materials inherit the advantage of highly efficient intersystem crossing of benzophenone-containing systems and generate a long-lived T_1 state of significant ^{3}LE nature from the naphthalene group. The present study demonstrates that it is still possible to achieve very long-lived RTP materials in benzophenone-containing systems despite the active nature of n–π* transitions in the organic systems. The detailed studies indicate that the key to achieving such long-lived RTP is to disrupt the contribution of n–π* transitions in the T_1 states.

With this understanding, we believe that the incorporation of suitable functional groups of low T_1 levels and ^{3}LE characters into benzophenone-containing systems would give rise to afterglow materials with even higher performances. Therefore, we believe that the present study provides a new, robust and practical pathway for fabricating long-lived RTP materials, which would have a significant impact in the corresponding research and application fields.

We acknowledge the financial support from the National Natural Science Foundation of China (22175194), the Shanghai Scientific and Technological Innovation Project (20QA1411600, 20ZR1469200), and the Hundred Talents Program from the Shanghai Institute of Organic Chemistry (Y121078).

Conflicts of interest

There are no conflicts to declare.

Notes and references

1 V. W.-W. Yam, V. K.-M. Au and S. Y.-L. Leung, *Chem. Rev.*, 2015, **115**, 7589–7728.
2 J. Mei, N. L. C. Leung, R. T. K. Kwok, J. W. Y. Lam and B. Z. Tang, *Chem. Rev.*, 2015, **115**, 11718–11940.
3 H. Uoyama, K. Goushi, K. Shizu, H. Nomura and C. Adachi, *Nature*, 2012, **492**, 234–238.
4 W. Zhao, Z. He and B. Z. Tang, *Nat. Rev. Mater.*, 2020, **5**, 869–885.
5 N. Gan, H. Shi, Z. An and W. Huang, *Adv. Funct. Mater.*, 2018, **28**, 1802657.
6 X. Ma, J. Wang and H. Tian, *Acc. Chem. Res.*, 2019, **52**, 738–748.
7 S. Hirata, *Adv. Opt. Mater.*, 2017, **5**, 1700116.
8 A. Forni, E. Lucenti, C. Botta and E. Cariati, *J. Mater. Chem. C*, 2018, **6**, 4603–4626.
9 Kenry, C. Chen and B. Liu, *Nat. Commun.*, 2019, **10**, 2111.
10 M. Singh, K. Liu, S. Qu, H. Ma, H. Shi, Z. An and W. Huang, *Adv. Opt. Mater.*, 2021, **9**, 2002197.
11 T. Zhang, X. Ma, H. Wu, L. Zhu, Y. Zhao and H. Tian, *Angew. Chem., Int. Ed.*, 2020, **59**, 11206–11216.
12 W. Jia, Q. Wang, H. Shi, Z. An and W. Huang, *Chem. – Eur. J.*, 2020, **26**, 4437–4448.
13 S. Guo, W. Dai, X. Chen, Y. Lei, J. Shi, B. Tong, Z. Cai and Y. Dong, *ACS Mater. Lett.*, 2021, **3**, 379–397.
14 S. Hirata, *Appl. Phys. Rev.*, 2022, **9**, 011304.
15 X. Yan, H. Peng, Y. Xiang, J. Wang, L. Yu, Y. Tao, H. Li and W. Huang, *Small*, 2022, **18**, e2104073.
16 H. Gao and X. Ma, *Aggregate*, 2021, **2**, e38.
17 Q. Li and Z. Li, *Acc. Chem. Res.*, 2020, **53**, 962–973.
18 G. Zhang, G. M. Palmer, M. W. Dewhirst and C. L. Fraser, *Nat. Mater.*, 2009, **8**, 747–751.
19 S. Hirata, K. Totani, J. Zhang, T. Yamashita, H. Kaji, S. R. Marder, T. Watanabe and C. Adachi, *Adv. Funct. Mater.*, 2013, **23**, 3386–3397.
20 Z. Yang, Z. Mao, X. Zhang, D. Ou, Y. Mu, Y. Zhang, C. Zhao, S. Liu, Z. Chi, J. Xu, Y.-C. Wu, P.-Y. Lu, A. Lien and M. R. Bryce, *Angew. Chem., Int. Ed.*, 2016, **55**, 2181–2185.
21 Z. Yang, C. Xu, W. Li, Z. Mao, X. Ge, Q. Huang, H. Deng, J. Zhao, F. L. Gu, Y. Zhang and Z. Chi, *Angew. Chem., Int. Ed.*, 2020, **59**, 17451–17455.
22 Y. Wang, J. Yang, M. Fang, Y. Yu, B. Zou, L. Wang, Y. Tian, J. Cheng, B. Z. Tang and Z. Li, *Matter*, 2020, **3**, 449–463.
23 D. Li, F. Lu, J. Wang, W. Hu, X.-M. Cao, X. Ma and H. Tian, *J. Am. Chem. Soc.*, 2018, **140**, 1916–1923.
24 Z.-Y. Zhang, Y. Chen and Y. Liu, *Angew. Chem., Int. Ed.*, 2019, **58**, 6028–6032.
25 X.-F. Wang, H. Xiao, P.-Z. Chen, Q.-Z. Yang, B. Chen, C.-H. Tung, Y.-Z. Chen and L.-Z. Wu, *J. Am. Chem. Soc.*, 2019, **141**, 5045–5050.
26 O. Bolton, K. Lee, H.-J. Kim, K. Y. Lin and J. Kim, *Nat. Chem.*, 2011, **3**, 205–210.
27 A. Fermi, G. Bergamini, R. Peresutti, E. Marchi, M. Roy, P. Ceroni and M. Gingras, *Dyes Pigm.*, 2014, **110**, 113–122.
28 J. Wang, X. Gu, H. Ma, Q. Peng, X. Huang, X. Zheng, S. H. P. Sung, G. Shan, J. W. Y. Lam, Z. Shuai and B. Z. Tang, *Nat. Commun.*, 2018, **9**, 2963.
29 X.-K. Ma, W. Zhang, Z. Liu, H. Zhang, B. Zhang and Y. Liu, *Adv. Mater.*, 2021, **33**, 2007476.
30 W. Z. Yuan, X. Y. Shen, H. Zhao, J. W. Y. Lam, L. Tang, P. Lu, C. Wang, Y. Liu, Z. Wang, Q. Zheng, J. Z. Sun, Y. Ma and B. Z. Tang, *J. Phys. Chem. C*, 2010, **114**, 6090–6099.
31 H. Ma, Q. Peng, Z. An, W. Huang and Z. Shuai, *J. Am. Chem. Soc.*, 2019, **141**, 1010–1015.
32 W. Zhao, Z. He, J. W. Y. Lam, Q. Peng, H. Ma, Z. Shuai, G. Bai, J. Hao and B. Z. Tang, *Chem*, 2016, **1**, 592–602.
33 Z. He, W. Zhao, J. W. Y. Lam, Q. Peng, H. Ma, G. Liang, Z. Shuai and B. Z. Tang, *Nat. Commun.*, 2017, **8**, 416.
34 S. M. A. Fateminia, Z. Mao, S. Xu, Z. Yang, Z. Chi and B. Liu, *Angew. Chem., Int. Ed.*, 2017, **56**, 12160–12164.
35 Y. Sun, J. Liu, J. Li, X. Li, X. Wang, G. Wang and K. Zhang, *Adv. Opt. Mater.*, 2022, **10**, 2101909.
36 X. Li, G. Wang, J. Li, Y. Sun, X. Deng and K. Zhang, *ACS Appl. Mater. Interfaces*, 2022, **14**, 1587–1600.
37 J. Liu, Y. Sun, G. Wang, X. Chen, J. Li, X. Wang, Y. Zou, B. Wang and K. Zhang, *Adv. Opt. Mater.*, 2022, **10**, 2201502.
38 J.-X. Wang, H. Zhang, L.-Y. Niu, X. Zhu, Y.-F. Kang, R. Boulatov and Q.-Z. Yang, *CCS Chem.*, 2020, **2**, 1391–1398.
39 S. Xu, W. Wang, H. Li, J. Zhang, R. Chen, S. Wang, C. Zheng, G. Xing, C. Song and W. Huang, *Nat. Commun.*, 2020, **11**, 4802.
40 S. Kuila and S. J. George, *Angew. Chem., Int. Ed.*, 2020, **59**, 9393–9397.
41 R. Kabe and C. Adachi, *Nature*, 2017, **550**, 384–387.
42 Y. Lei, W. Dai, J. Guan, S. Guo, F. Ren, Y. Zhou, J. Shi, B. Tong, Z. Cai, J. Zheng and Y. Dong, *Angew. Chem., Int. Ed.*, 2020, **59**, 16054–16060.
43 C. Chen, Z. Chi, K. C. Chong, A. S. Batsanov, Z. Yang, Z. Mao, Z. Yang and B. Liu, *Nat. Mater.*, 2021, **20**, 175–180.
44 X. Wang, Y. Sun, G. Wang, J. Li, X. Li and K. Zhang, *Angew. Chem., Int. Ed.*, 2021, **60**, 17138–17147.
45 Y. Pan, J. Li, X. Wang, Y. Sun, J. Li, B. Wang and K. Zhang, *Adv. Funct. Mater.*, 2022, **32**, 2110207.
46 G. Wang, J. Li, X. Li, X. Wang, Y. Sun, J. Liu and K. Zhang, *Chem. Eng. J.*, 2022, **431**, 134197.
47 G. Wang, X. Chen, J. Liu, S. Ding and K. Zhang, *Sci. China: Chem.*, 2022, DOI: 10.1007/s11426-022-1432-y.

